Electronic Supplementary Material (ESI) for Soft Matter.

Ionic N-Phenylpyridinium Tetracatenar Mesogens: Competing Driving Forces in Mesophase Formation and Unprecedented Difference in Phase Stabilisation within an Homologous Series

Jordan D. Herod, Martin A. Bates, Adrian C. Whitwood and Duncan W. Bruce*

Department of Chemistry

University of York

Heslington

YORK YO10 5DD (UK)

Tel: (+44) 1904 324085

E-mail: duncan.bruce@york.ac.uk

Supplementary Information

Nuclear Magnetic Resonance (NMR):

^{1}H NMR spectra were obtained on Jeol ECS400 and ECX400 with a field strength 400 MHz, equipped with a sample changer. ^{13}C NMR spectra were obtained on a Jeol ECS400 with a frequency of 101 MHz, equipped with a sample changer. ^{19}F NMR were collected on a Jeol ECS400 with a frequency of 376 MHz, equipped with a sample changer.

Polarised Optical Microscopy (POM):

Liquid crystal textures were observed using an Olympus BX50 Optical Microscope equipped with a Linkam Scientific LTS350 heating stage, Linkam LNP2 cooling pump and a Linkam TMS92 controller.

Differential Scanning Calorimetry (DSC):

Calorimetry scans were run on a Mettler Toledo DSC822e, (running on a Stare software) equipped with a TSO801R0 sample robot and calibrated using pure indium. Samples were run at heating/cooling rates of 5 °C min^{-1}. DSC data mentioned in the article are onset temperatures.

Elemental Analysis:

Analysis was carried out on an Exeter Analytical Inc CE 440 Elemental Analyzer and a Sartorius SE2 analytical balance by Dr Graeme McAllister at the University of York.

Small-Angle X-ray Scattering (SAXS):

Small angle X-ray scattering was performed using a Bruker D8 Discover equipped with a temperature controlled, bored graphite rod furnace, custom built at the University of York. The radiation used was copper Kα (λ = 0.154056 nm) from a 1 µS microfocus source. Diffraction patterns were recorded on a 2048x2048 pixel Bruker VANTEC 500 area detector set at a distance of 121 mm from the sample. Samples were filled into 0.9 mm capillary tubes and aligned with a pair of 1 T magnets, with the field strength at the sample position being approximately 0.6 T. Diffraction patterns were collected as a function of temperature. Two-dimensional scattering patterns were collected every 10 °C on heating to the isotropic liquid and subsequent cooling to room temperature at a rate of 10 °C min^{-1}. The data were then processed using Origin.

Single Crystal X-ray Diffraction

Diffraction data were collected at 110 K on an Oxford Diffraction SuperNova dual-source X-ray diffractometer with CuKα (λ = 1.54184) radiation using an EOS CCD camera. The crystal was cooled with an Oxford Instruments Cryojet. Diffractometer control, data collection, initial unit cell determination, frame integration and unit-cell refinement was carried out with 'Crysalis'.[a] Face-indexed absorption corrections were applied using spherical harmonics, implemented in SCALE3 ABSPACK scaling algorithm.[27] OLEX2[b] was used for overall structure solution, refinement and preparation of computer graphics and publication data. Within OLEX2, the algorithm used for structure solution was ShelXT[c] Refinement by full-matrix least-squares used the SHELXL-97[d] algorithm within OLEX2. All non-hydrogen atoms were refined anisotropically. Hydrogen atoms were placed using riding models and included in the refinement at calculated positions.

References

a CrysAlisPro, Oxford Diffraction Ltd. Version 1.171.34.41.

b Empirical absorption correction using spherical harmonics, implemented in SCALE3 ABSPACK scaling algorithm within CrysAlisPro software, Oxford Diffraction Ltd. Version 1.171.34.40

c O. V. Dolomanov, L. J. Bourhis, R. J. Gildea, J. A. K. Howard, H. Puschmann, *J. Appl. Crystallogr.* **2009**, *42*, 339-341.

d G. Sheldrick, *Acta Crystallogr. A*, **2008**, *64*, 112-122.

Synthetic Procedures

The following procedures document the preparation of octyloxy homologues. The methods for the preparation of other homologues are identical.

Preparation of **1:**

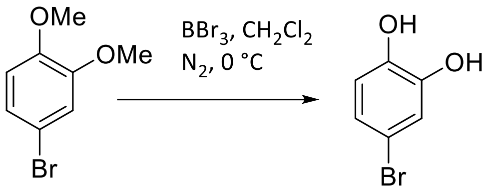

To a three-necked round bottom flask purged with nitrogen was added 4-bromoveratrole (6.61 ml, 46 mmol) and anhydrous CH_2Cl_2 (200 ml). The solution was cooled to 0 °C under a flow of nitrogen and BBr_3 (101 ml, 101 mmol, 1 mol dm^{-3} in dichloromethane) added drop wise. The reaction mixture was then stirred at 0 °C for a further 10 min before being allowed to warm to RT and stirred for a further hour, after which time the reaction was quenched with water (200 ml) and the biphasic mixture separated. The aqueous layer was extracted with dichloromethane (3 x 150 ml) and the combined organic layers dried over $MgSO_4$ and the solvent removed to leave a grey oil that slowly crystallised with time (90%): ^{1}H NMR (400 MHz, $CDCl_3$) 7.02 (a, 1H, d, *J* = 2.5 Hz), 6.92 (b, 1H, dd, *J* = 8.5, 2.5 Hz), 6.74 (c, 1H, d, *J* = 8.5 Hz), 5.63 (1H, s), 5.44 (1H, s).

Preparation of **2**-8:

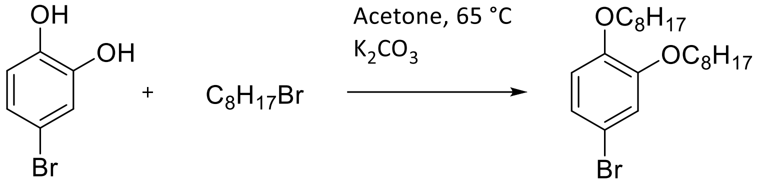

3,4-Dihydroxybromobenzene (7.8 g, 41.3 mmol) was dissolved in acetone (200 ml) and to this solution was added potassium carbonate (11.4 g, 82.6 mmol) and 1-bromooctane (14.5 g, 13.0 ml, 75.1 mmol); the resulting suspension was heated under reflux for 2 days. The reaction mixture was then cooled to room temperature, diluted with CH_2Cl_2 (150 ml) to prevent the product from crystallising and the residual potassium carbonate removed via filtration. The filtrate was then evaporated to dryness and the residue taken into diethyl ether (200 ml), washed with aqueous NaOH (200 ml, 10 wt%), water (200 ml) and aqueous NaCl (200 ml, saturated). The organic layer was then dried over $MgSO_4$ and the solvent removed. The product was crystallised from hot acetone to leave a colourless microcrystalline solid (51%): ^{1}H NMR for **2**-*8* (400 MHz, $CDCl_3$) δ 6.98 (2H, m), 6.73 (1H, d, *J* = 9.0 Hz), 3.96 (2H, t, *J* = 6.5 Hz), 3.95 (2H, t, *J* = 6.5 Hz), 1.79 (4H, m), 1.45 (4H, m), 1.30 (16H, m), 0.88 (6H, t, *J* = 7.0 Hz).

Preparation of **3**-8:

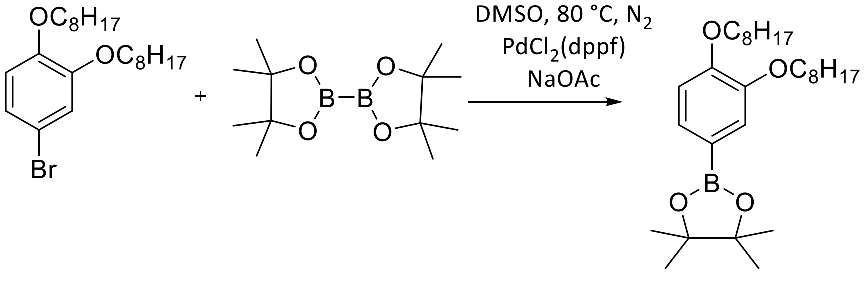

A three-necked round bottom flask purged with N_2 was charged with **2**-8 (2.47 g, 5.98 mmol) and dissolved in anhydrous DMSO (40 ml). *Bis*-pinacolato diboron (1.82 g, 7.17 mmol) and NaOAc (1.47 g, 17.9 mmol) were added and the reaction mixture heated to 80 °C under a flow of N_2. [$PdCl_2$(dppf)] (0.15g, 0.18mmol, 3 mol%) was then added and the resulting solution stirred at 80 °C for 16 h. The reaction mixture was cooled to room temperature, diluted with water (100 ml) and the product extracted into diethyl ether (4 x 100 ml). The combined organic layers were then washed repeatedly with water (5 x 150 ml) to remove any residual DMSO, dried over $MgSO_4$ and the solvent removed under reduced pressure. The product was purified *via* column chromatography on silica gel using 40-60 °C petroleum spirit:ethyl acetate (9:1) to afford a colourless solid (54%): ^{1}H NMR (400 MHz, $CDCl_3$) δ 7.38 (1H, dd, *J* = 8.0, 1.5 Hz), 7.29 (1H, d, *J* = 1.5 Hz), 6.87 (1H, d, *J* = 8.0 Hz), 4.04 (2H, t, J = 6.5 Hz), 4.02 (2H, t, *J* = 6.5 Hz), 1.81 (4H, m), 1.46 (4H, m), 1.33 (12H, s), 1.26 (16H, m), 0.88 (6H, m).

Preparation of **4**-8:

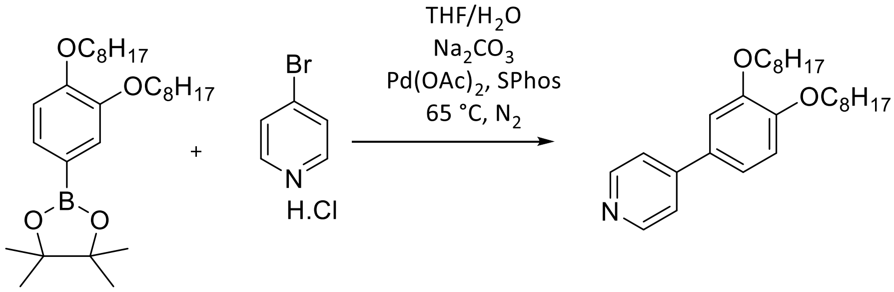

A three-necked round bottomed flask purged with N_2 was charged with **3**-8 (4.0 g, 8.70 mmol) and dissolved in anhydrous THF (50 ml). To this solution was added 4-bromopyridine hydrochloride (1.86 g, 9.57 mmol) and aqueous Na_2CO_3 (50 ml, 2 mol dm^{-3}); the biphasic mixture was then sparged under a flow of argon for 10 min whilst being agitated in an ultrasonic bath. The reaction mixture was heated at 65 °C under a flow of N_2 and the pre-prepared catalyst in THF added (7.14 x 10^{-2} mmol, 1 mol%). The catalyst was prepared by dissolving [$Pd(OAc)_2$] (0.019 g, 8.7 x 10^{-2} mmol, 1 mol%) and SPhos (0.036 g, 8.7 x 10^{-2} mmol, 1 mol%) in anhydrous THF (2 ml) and stirring briefly under N_2 until the mixture turned deep red. The reaction was monitored *via* TLC (CH_2Cl_2:MeOH, 95:5) and after complete consumption of the starting materials the reaction mixture was cooled to room temperature and the biphasic mixture separated. The aqueous layer was extracted with dichloromethane (3 x 100 ml) and the combined organic layers dried over $MgSO_4$ and the solvent removed. The product was then crystallised from hot *n*-hexane to afford a colourless, microcrystalline solid (84%): ^{1}H NMR (400 MHz, $CDCl_3$) δ 8.61 (2H, AA'XX', *J* = 6.0 Hz), 7.46 (2H, AA'XX', *J* = 6.0 Hz), 7.20 (1H, dd, *J* = 8.5, 2.5 Hz), 7.16 (1H, d, *J* = 2.5 Hz), 6.96 (1H, d, *J* = 8.5 Hz), 4.08 (2H, t, *J* = 6.5 Hz), 4.05 (2H, t, *J* = 6.5 Hz), 1.85 (4H, m), 1.48 (4H, m), 1.30 (16H, m), 0.88 (6H, t, *J* = 6.5 Hz).

Preparation of **5**-8:

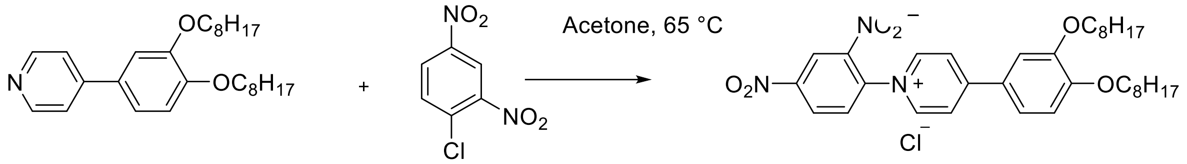

Phenylpyridine **4**-8 (3.25 g, 7.91 mmol) was taken into acetone (75 ml) and 1-chloro-2,4-dinitrobenzene (1.76 g, 8.7 mmol) was added; the resulting suspension was heated under reflux for 4 days. The reaction mixture was then cooled to room temperature and the orange precipitate isolated *via* filtration and washed repeatedly with acetone: ^{1}H NMR (400 MHz, CD_3OD) δ 9.25 (1H, d, *J* = 2.5 Hz), 9.02 (2H, AA'XX', *J* = 9.0 Hz), 8.88 (1H, dd, *J* = 8.5, 2.5 Hz), 8.58 (2H, AA'XX', *J* = 7.0 Hz), 8.26 (1H, d, *J* = 8.5 Hz), 7.82 (1H, dd, *J* = 8.5, 2.5 Hz), 7.69 (1H, d, *J* = 2.5 Hz), 7.20 (1H, d, *J* = 9.0 Hz), 4.16 (2H, t, *J* = 6.5 Hz) 4.15 (2H, t, *J* = 6.5 Hz), 1.84 (4H, m), 1.54 (4H, m), 1.33 (16 H), 0.87 (6H, t, *J* = 7.0 Hz).

Preparation of **6**-8:

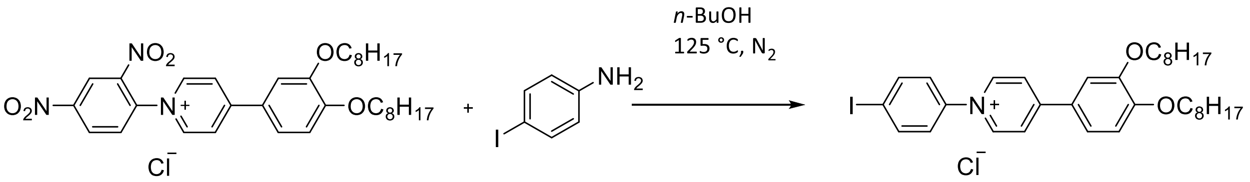

A three-necked round bottomed flask purged with nitrogen was charged with Zincke salt **5**-8 (0.25 g, 0.41 mmol) and dissolved in *n*-butanol (6 ml). 4-iodoaniline (0.36 g, 1.64 mmol) was added and the resulting suspension heated under reflux for 16 h after which time the reaction mixture had become a deep yellow solution. The solution was cooled to room temperature and the resulting precipitate was isolated *via* filtration, triturated with cold dichloromethane and acetone and dried (53%): ^{1}H NMR (400 MHz, DMSO-*d*) δ 9.19 (2H, AA'XX', *J* = 7.0 Hz), 8.64 (2H, AA'XX', *J* = 7.0 Hz), 8.13 (2H, AA'XX', *J* = 8.5 Hz), 7.86 (1H, dd, *J* = 8.5, 2.0 Hz), 7.74 (1H, d, *J* = 2.0 Hz), 7.68 (2H, AA'XX', *J* = 8.5 Hz), 7.21 (1H, d, *J*= 8.5 Hz), 4.14, (2H, t, *J* = 6.5 Hz) 4.12 (2H, t, *J* = 6.5 Hz), 1.75 (4H, m), 1.45 (4H, m), 1.30 (16H, m), 0.85 (3H, t, *J* = 7.0 Hz).

Preparation of **7**-8:

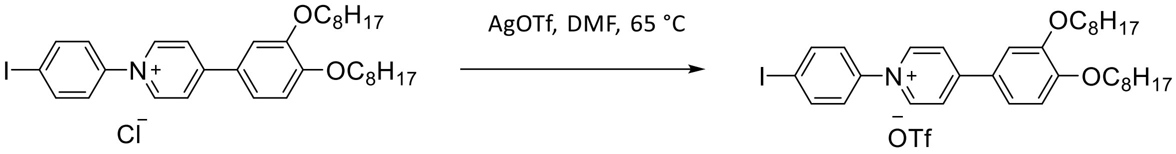

Chloride salt **6**-8 (0.42 g, 0.65 mmol) was taken into DMF (80 ml) and the resulting solution heated to 65 °C. Silver triflate (0.42 g, 1.62 mmol) was then added after which time a yellow suspension immediately formed; the reaction mixture was stirred at 65 °C for 16 h before being cooled to room temperature and the precipitate removed. The filtrate was then evaporated to dryness and the residue taken into CH_2Cl_2 (50 ml), washed repeatedly with water (4 x 75 ml) and dried over $MgSO_4$. The solvent was removed under reduced pressure and the compound subsequently crystallised from hot EtOH to yield a yellow solid (58%): ^{1}H NMR (400 MHz, DMSO-*d*) δ 9.19 (2H, AA'XX', *J* = 7.0 Hz), 8.64 (2H, AA'XX', *J* = 7.0 Hz), 8.13 (2H, AA'XX', *J* = 8.5 Hz), 7.86 (1H, dd, *J* = 8.5, 2.0 Hz), 7.74 (1H, d, *J* = 2.0 Hz), 7.68 (2H, AA'XX', *J* = 8.5 Hz), 7.21 (1H, d, *J*= 8.5 Hz), 4.14 (2H, t, *J* = 6.5 Hz) 4.11 (2H, t, *J* = 6.5 Hz), 1.75 (4H, m), 1.45 (4H, m), 1.30 (16 H, m), 0.85 (3H, t, *J* = 7.0 Hz).

Preparation of **8**-8:

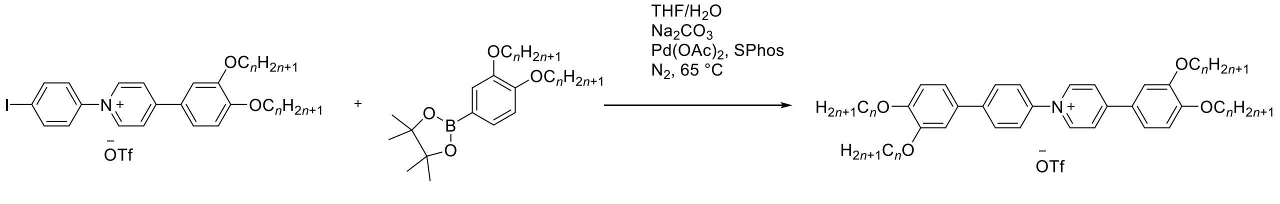

A three-necked round bottomed flask purged with nitrogen was charged with triflate salt **7**-*8* (0.25 g, 0.33 mmol) and anhydrous THF (15 ml). To this yellow solution was added borate ester **3**-*8* (0.18 g, 0.39 mmol) and aqueous sodium carbonate (15 ml, 2 mol dm^{-3}). Argon was then bubbled through the biphasic mixture whilst undergoing agitation in an ultrasonic bath to rigorously remove oxygen from the reaction mixture.

[$Pd_3(OAc)_6$] (7.4 x 10^{-4} g, 3.3 x 10^{-3} mmol) and SPhos (1.35 x 10^{-3} g, 3.3 x 10^{-3} mmol) were dissolved in anhydrous THF (1 ml) and stirred under nitrogen until the mixture became red. This pre-prepared catalyst was then added to the reaction mixture, which was then heated to 65 °C under a steady flow of nitrogen. On complete consumption of the limiting reagent (after 16 h), the reaction was cooled to room temperature, the biphasic mixture separated and the aqueous layer extracted with CH_2Cl_2 (2 x 25 ml). The combined organic layers were dried over $MgSO_4$ and the solvent removed under reduced pressure. The product was purified by flash column chromatography on silica gel (eluent CH_2Cl_2:MeOH, 95:5) and subsequently crystallised from hot ethanol to afford a yellow microcrystalline solid: ^{1}H NMR (400 MHz, $CDCl_3$) δ 8.80 (2H, AA'XX', *J* = 7.0 Hz), 8.25 (2H, AA'XX', *J* = 7.0 Hz), 7.41 (1H, dd, *J* = 8.0, 2.0 Hz), 7.31 (1H, d, *J* = 2.0 Hz), 7.03 (1H, d, *J* = 2.0 Hz), 7.00 (1H, dd, *J* = 8.0, 2.0 Hz), 6.84 (1H, d, *J* = 8.0 Hz), 6.81 (1H, d, *J* = 8.0 Hz), 4.06 (2H, t, *J* = 7.0 Hz), 4.01 (2H, t, *J* = 7.0 Hz), 3.97 (2H, t, *J* = 7.0 Hz), 3.90 (2H, t, *J* = 7.0 Hz), 1.82 (8H, m), 1.47 (8H, m), 1.29 (32H, m), 0.85 (12H, m). ^{19}F NMR (376 MHz, $CDCl_3$) δ -78.09, (s). ^{13}C NMR (101 MHz, $CDCl_3$) δ 14.22, 22.80, 22.06, 26.15, 26.18, 26.21, 29.10, 29.40, 29.43, 29.52, 29.57, 31.96, 69.17, 69.25, 69.58, 69.63, 112.01, 112.55, 113.10, 113.72, 119.90, 120.93 (J_{CF} = 320 Hz), 122.60, 123.58, 124.06, 124.59, 125.71, 128.58, 130.84, 139.79, 142.50, 144.00, 149.61, 150.03, 153.99, 155.99.

The NMR data presented for **8**-8 are indicative of the NMR data for all derivatives, only the integrations for hydrogen atoms in the aliphatic chains vary. Elemental analyses for all compounds from **8**-8 to **8**-18 are presented in Table S2.

Table S1. Thermal data for the new pyridinium salts (values from polarising optical microscopy).

Compound	**Transition**	***T* / °C**
8-8	Crys – SmA	114
	SmA -Iso	169
8-10	Crys – Crys'	74
	Crys' – SmA	118
	SmA -Iso	161
8-12	Crys - Crys'	79
	Crys – SmA	120
	SmA -Iso	143
8-13	Crys - Crys'	95
	Crys – SmA	120
	SmA -Iso	141
8-14	Crys - Col_h	118
	Col_h – Iso*	210
8-16	Crys - Col_h	117
	Col_h – Iso*	207
8-18	Crys - Crys'	101
	Crys - Col_h	109
	Col_h – Iso*	199

* Apparent clearing points, although there is evidence of decomposition by these temperatures.

Table S2. Elemental analyses of compounds **8**-*n* (theoretical values in parentheses).

Compound	%C	%H	%N
8-8	69.4 (69.3)	8.7 (8.5)	1.5 (1.4)
8-10	70.9 (71.0)	9.2 (9.1)	1.2 (1.2)
8-12	72.3 (72.4)	9.6 (9.6)	1.2 (1.2)
8-13	72.5 (73.0)	10.2 (9.8)	1.0 (1.1)
8-14	73.6 (73.5)	10.3 (10.0)	1.0 (1.1)
8-16	74.7 (74.5)	10.4 (10.4)	1.3 (1.0)
8-18	75.0 (75.3)	10.7 (10.7)	1.3 (0.9)

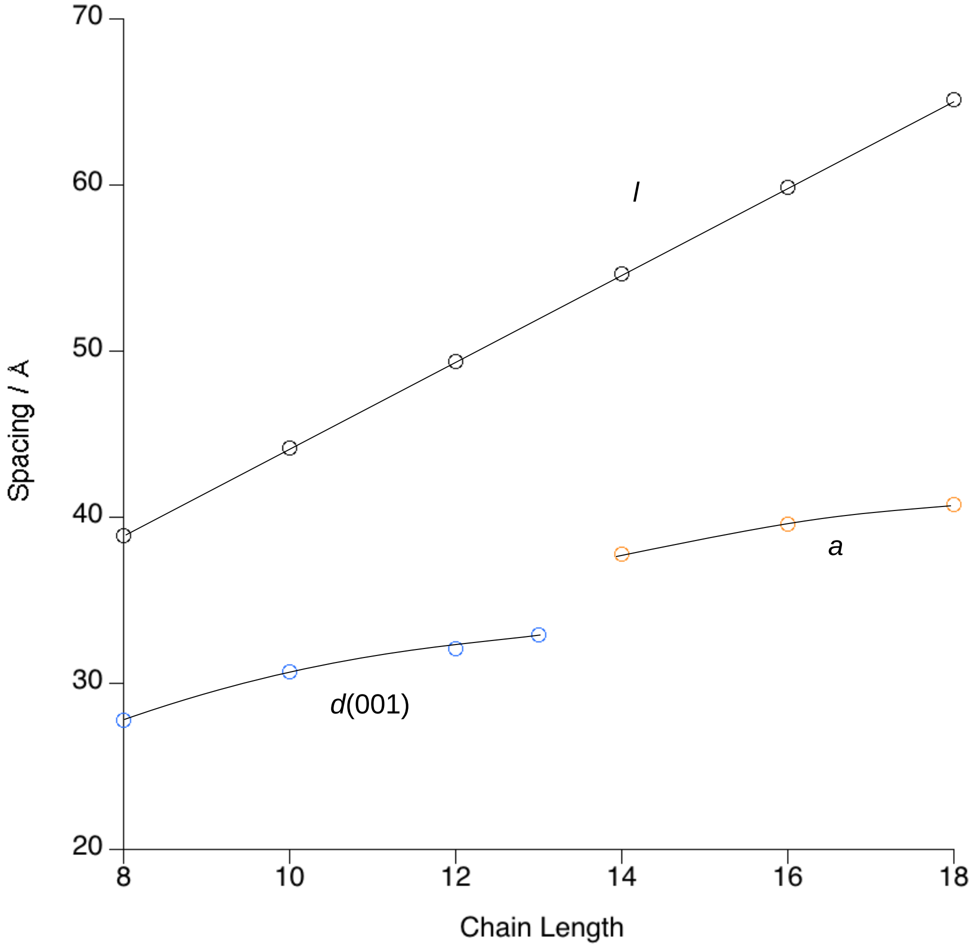

Figure S1 The *d*(001) distance, the lattice parameter (*a*) and cation length (*l*) for compounds **8**-*n*. Both *a* and *d*(100) were obtained from SAXS measurements at a reduced temperature of 0.97

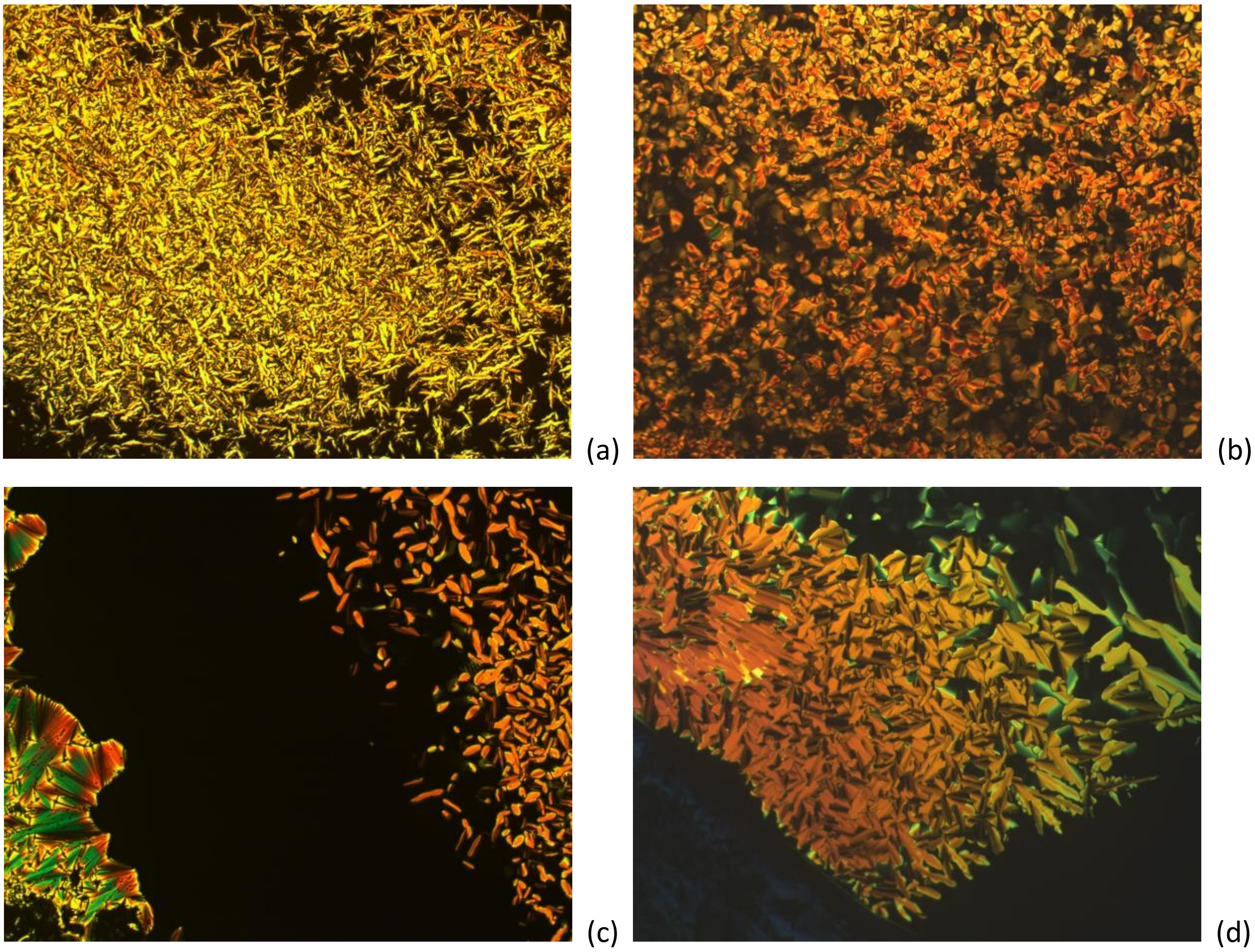

Figure S2. Optical micrographs of: (a) **8**-14 at 126 °C on cooling, (b) contact preparation between **8**-16 (LHS) and **8**-14 (RHS) at 181 °C showing continuous miscibility, (c) contact preparation between **8**-12 (LHS) and **8**-14 (RHS) at 123 °C showing miscibility gap, (d) **8**-14 at 128 °C obtained by slow evaporation of a DMF solution.

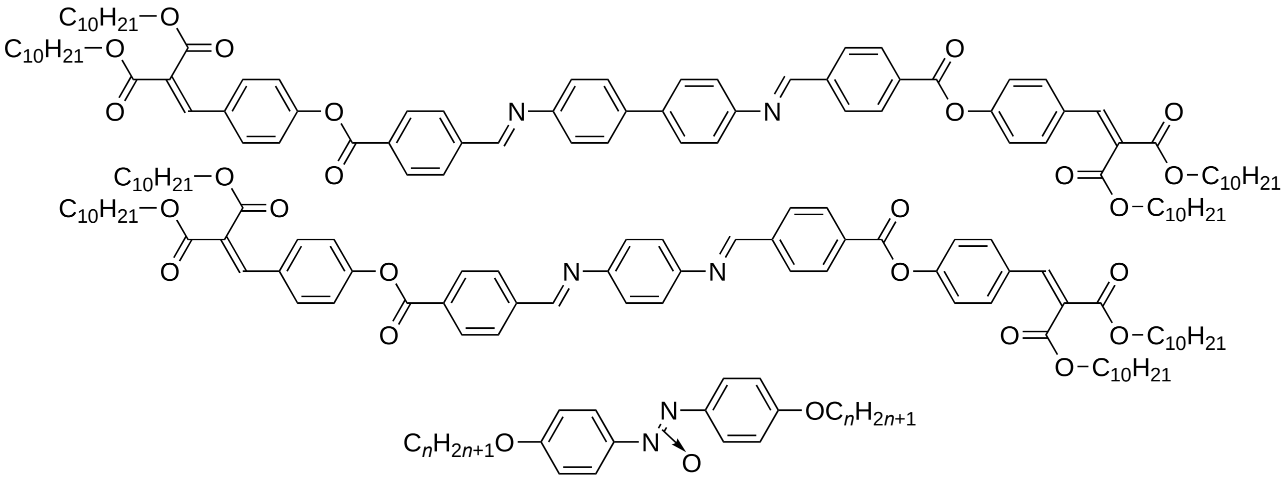

Figure S3. The two 'swallow-tailed' compounds and the small, calamitic mesogen used in the mixture studies by Pelzl *et al.*

(G. Pelzl, S. Diele, K. Ziebarth, W. Weissflog and D. Demus, *Liq. Cryst.*, **1990**, *8*, 765–773.)

Calculations

DFT calculations for the cation were run using Gaussian 16^{e} using the B3LYP functional and 6-311G(d,p) basis set.

The dihedral angles between the four rings were found to be ≈ ±22°, ±52° and ±34°, respectively. Due to these being local minima, calculations were run for the n = 1 analogue with dihedral angles of different signs between the four rings.The resulting solutions differ by approximately 1 kJ mol^{-1}. The minimum was found to be +22°, –52° and –34°. The same calculations were run for n = 2, 4 and 8. The Mulliken charges and ESP map were found to be very similar for all, the charges for n = 8 differing by about ±0.02 for the oxygen atoms and neighbouring carbons from their values for the methyl analogue (n = 1).

Calculations (see also Fig S3) were also run for the uncharged system of the combined cation and anion. These were run ten times from different starting points and orientations for the anion (including configurations were the anion was close to each ring in turn) and in each case the anion is eventually found in the pocket next to the pyridine ring, being always to the side rather than directly above, with two or all three oxygen atoms close to the ring.

Reference

e *Gaussian 16, Revision B.01*, M. J. Frisch, G. W. Trucks, H. B. Schlegel, G. E. Scuseria, M. A. Robb, J. R. Cheeseman, G. Scalmani, V. Barone, G. A. Petersson, H. Nakatsuji, X. Li, M. Caricato, A. V. Marenich, J. Bloino, B. G. Janesko, R. Gomperts, B. Mennucci, H. P. Hratchian, J. V. Ortiz, A. F. Izmaylov, J. L. Sonnenberg, D. Williams-Young, F. Ding, F. Lipparini, F. Egidi, J. Goings, B. Peng, A. Petrone, T. Henderson, D. Ranasinghe, V. G. Zakrzewski, J. Gao, N. Rega, G. Zheng, W. Liang, M. Hada, M. Ehara, K. Toyota, R. Fukuda, J. Hasegawa, M. Ishida, T. Nakajima, Y. Honda, O. Kitao, H. Nakai, T. Vreven, K. Throssell, J. A. Montgomery, Jr., J. E. Peralta, F. Ogliaro, M. J. Bearpark, J. J. Heyd, E. N. Brothers, K. N. Kudin, V. N. Staroverov, T. A. Keith, R. Kobayashi, J. Normand, K. Raghavachari, A. P. Rendell, J. C. Burant, S. S. Iyengar, J. Tomasi, M. Cossi, J. M. Millam, M. Klene, C. Adamo, R. Cammi, J. W. Ochterski, R. L. Martin, K. Morokuma, O. Farkas, J. B. Foresman, and D. J. Fox, Gaussian, Inc., Wallingford CT, 2016.

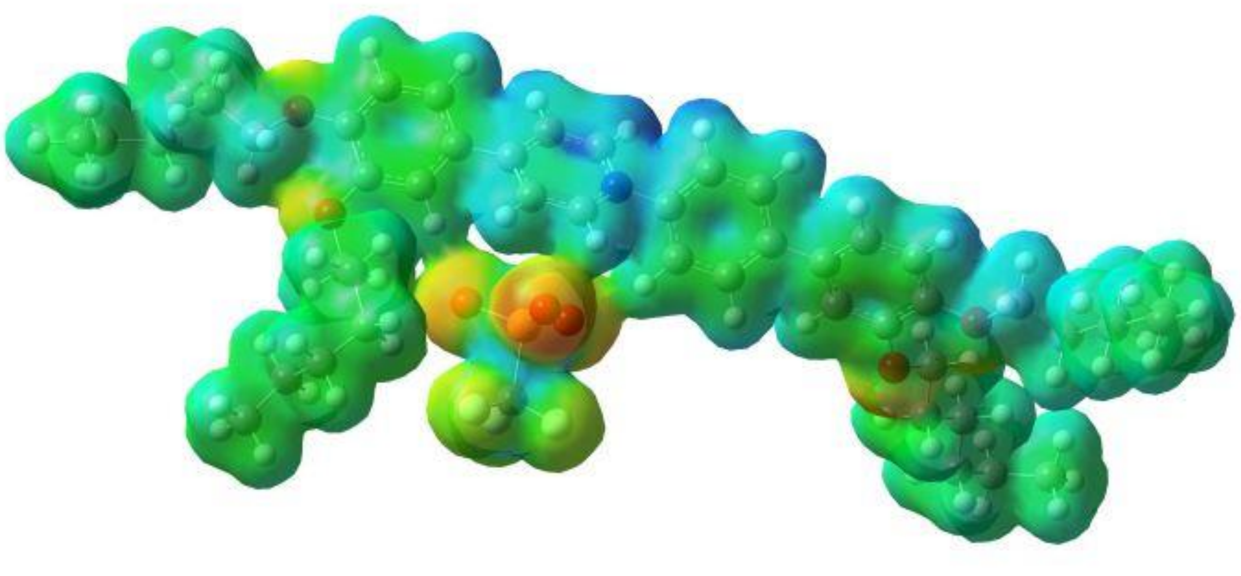

Figure S4. A snapshot from the calculations of the cation and anion system (*n* = 6) showing the location of the anion close to the area of greatest positive electrostatic potential – the pyridinium ring.

X-Ray Single Crystal Structure

One of the octyl side chains was disordered and modelled in two positions with refined occupancies of 0.714:0.286(4). The C-C bond lengths in the disordered part of the chain were restrained to be 1.54 angstroms except for the terminal C-C bond lengths which were restrained to be 1.52 Å. Two pairs of ADPs in the disordered chains were constrained to be equal, namely: C26 & C26a and C28 & C28a.

The triflate anion/water showed minor disorder with the triflate being modelled in two positions with refined occupancies of 0.9598:0.0402(15). For the minor form, the C-F bond lengths were restrained to be 1.33 Å, the S-O bond lengths restrained to be 1.44 Å and the C-S bond length restrained to be the same as that of the major form. ADP of O5A was constrained to be equal to that of O5 and the ADP of C56a, F1a, F2a, F3a, O6a, O7a were restrained to be approximately isotropic.

Figures below have disorder removed for clarity, but if this is of interest then the cif file is available.

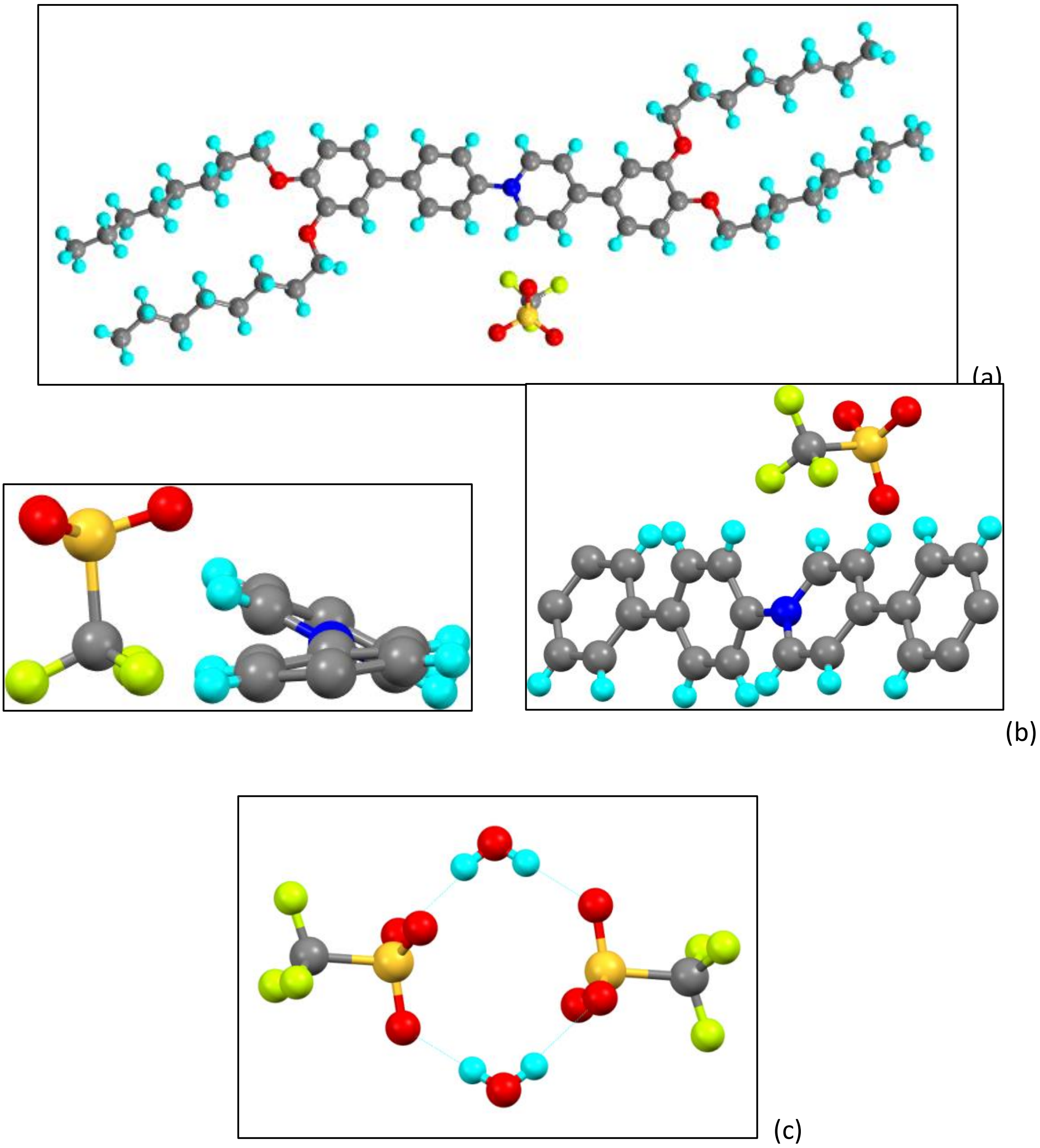

Figure S5. (a) Top view and (b) end-on and side views (terminal rings and all chains removed for clarity) of the molecular structure of **8**-8. There appear to be no specific interactions between the pyridinium hydrogen atoms and the triflate oxygen atoms, *but* the structure contains a molecule of water (not shown in (a) and (b) for clarity) which forms a '2+2' hydrogen-bonded 'adduct' (c) of two water molecules and two triflate anions.

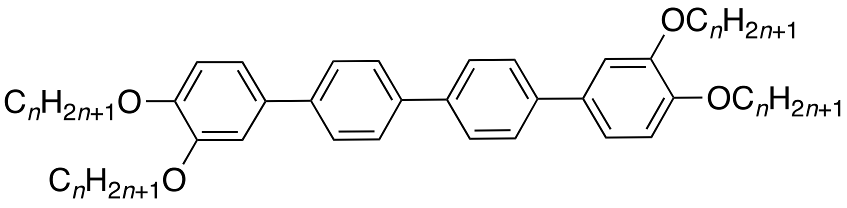

Figure S6. Neutral analogue of **8**-*n* as described by Sultana *et al.*

(N. H. Sultana, S. M. Kelly, B. Mansoor and M. O'Neill, *Liq. Cryst.*, **2007**, *34*, 1307-1316.)[‡]

[‡] Here, we re-made the homologues with *n* = 1 and 12 and then made the homologue with *n* = 8. The original publication reported homologues with *n* = 1, 5 and 12 and so the new *n* = 8 homologue ought also to have been columnar. In our hands, the *n* = 1 homologue was simply crystalline melting at 299 °C (Lit. Cr – 278 • Col • 294 • Iso) as was the new *n* = 8 homologues which melted at 167 °C. For *n* = 12 we could confirm the existence of a columnar phase, even if we could not reproduce the reported temperatures (**this work:** Crys • 144 • $\mathrm{Col_h}$ • 149 • Iso; **Lit.** Crys • 125 • $\mathrm{Col_h}$ • 155 • Iso).

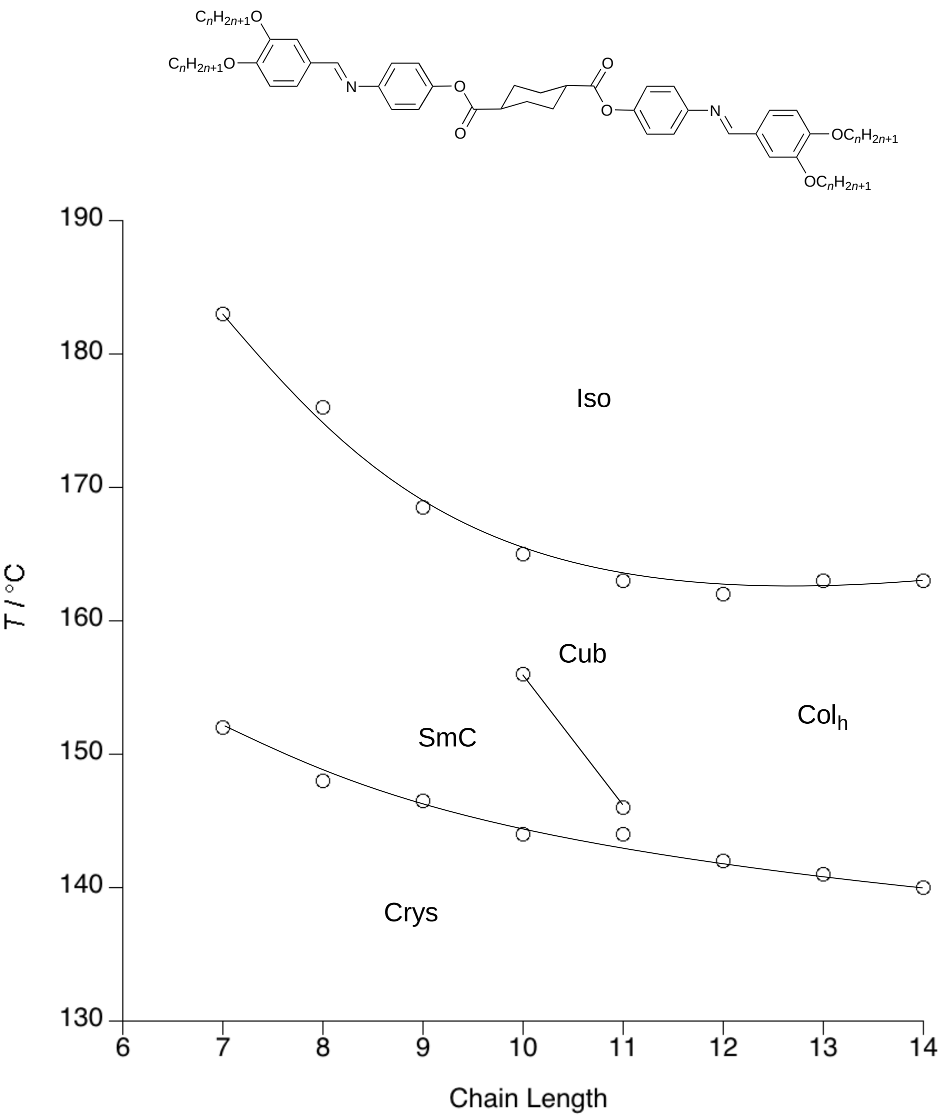

Figure S7. Transition temperatures plotted from data given in
M. Gharbia, A. Gharbi, H. T. Nguyen, J. Malthête, *Curr. Opin. Colloid. Interfac. Sci.*, **2002**, *7*, 312-325.

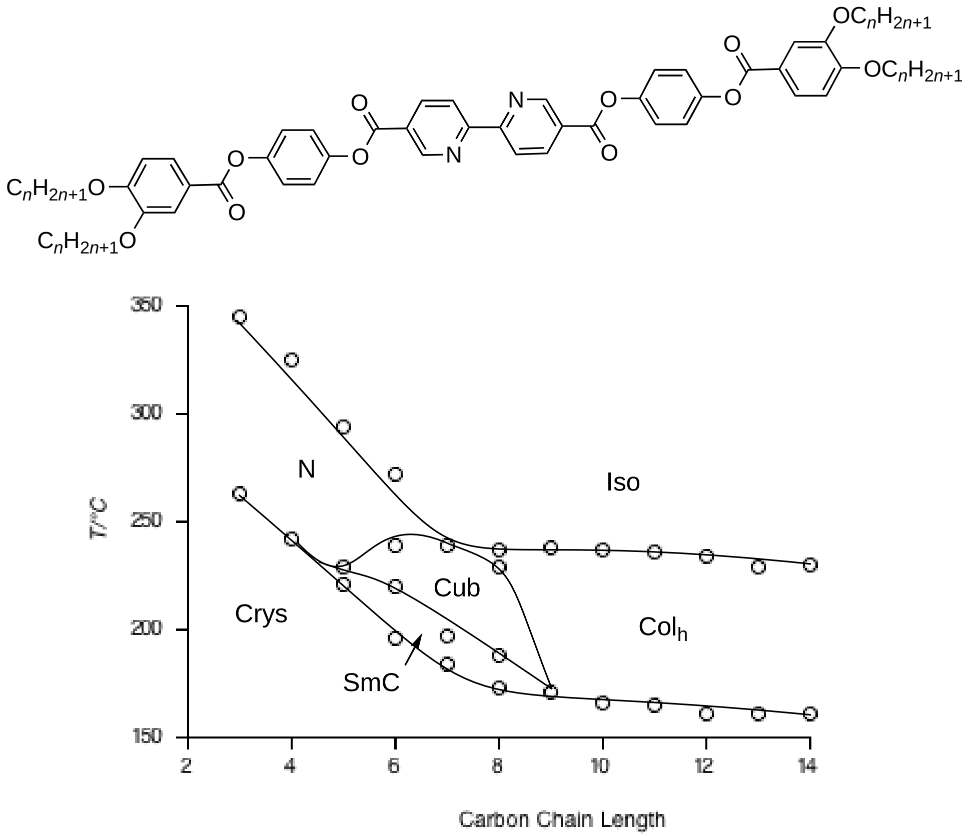

Figure S8. Phase diagram for tetracatenar bipyridines – figure adapted from D. W. Bruce, *Acc. Chem. Res.*, **2000**, *33*, 831-840.

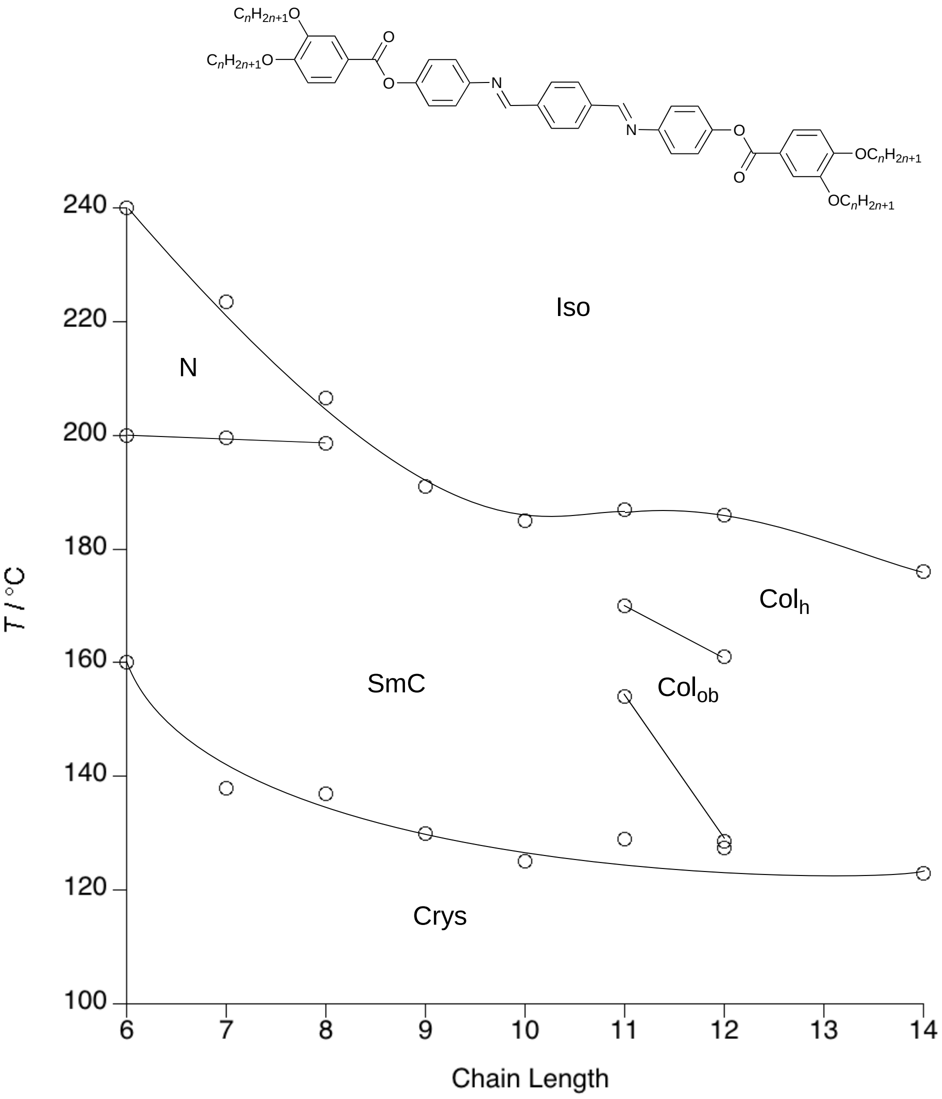

Figure S9. Transition temperatures plotted from data given in

M. Gharbia, A. Gharbi, H. T. Nguyen, J. Malthête, *Curr. Opin. Colloid. Interfac. Sci.*, **2002**, *7*, 312-325.

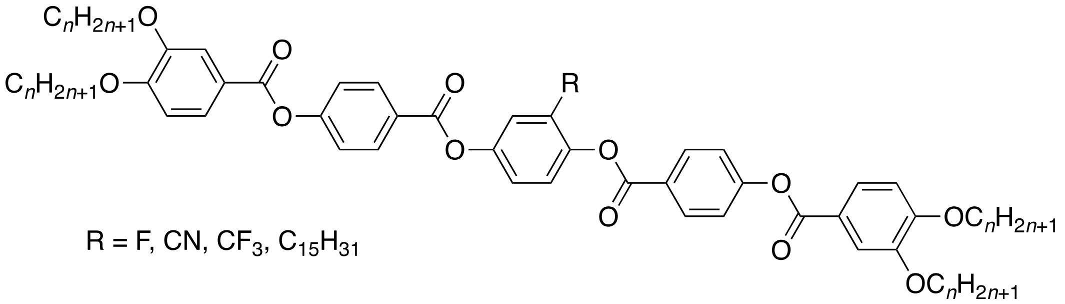

Figure S10 Tetracatenar liquid crystals with covalent lateral substituents.

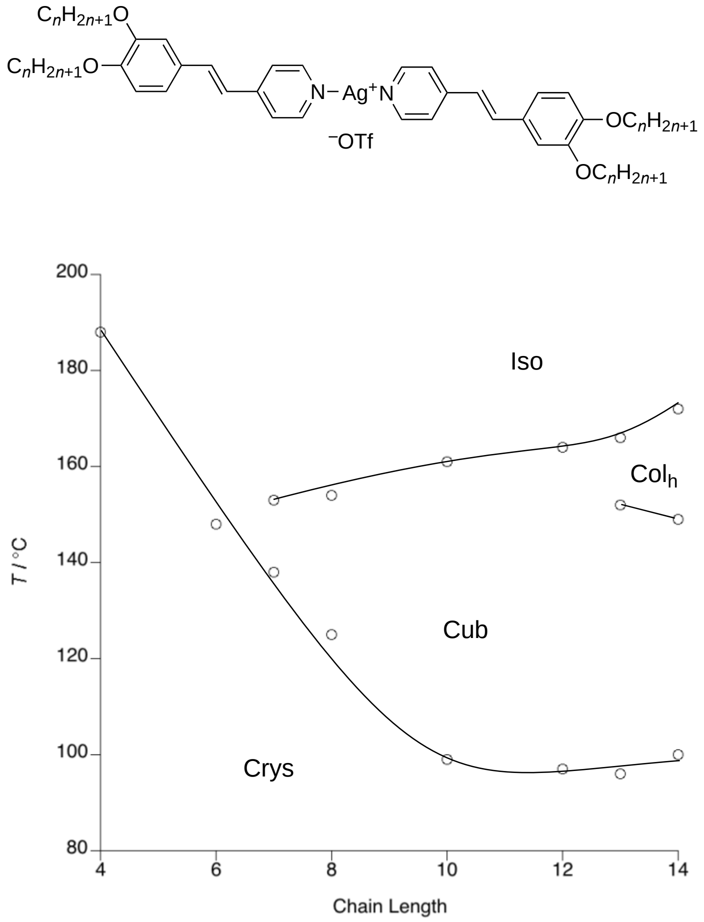

Figure S11. Phase diagram for tetracatenar silver(I) stilbazole triflate complexes – figure re-drawn from data in B. Donnio and D. W. Bruce, *New J. Chem.*, **1999**, *23*, 275-286.

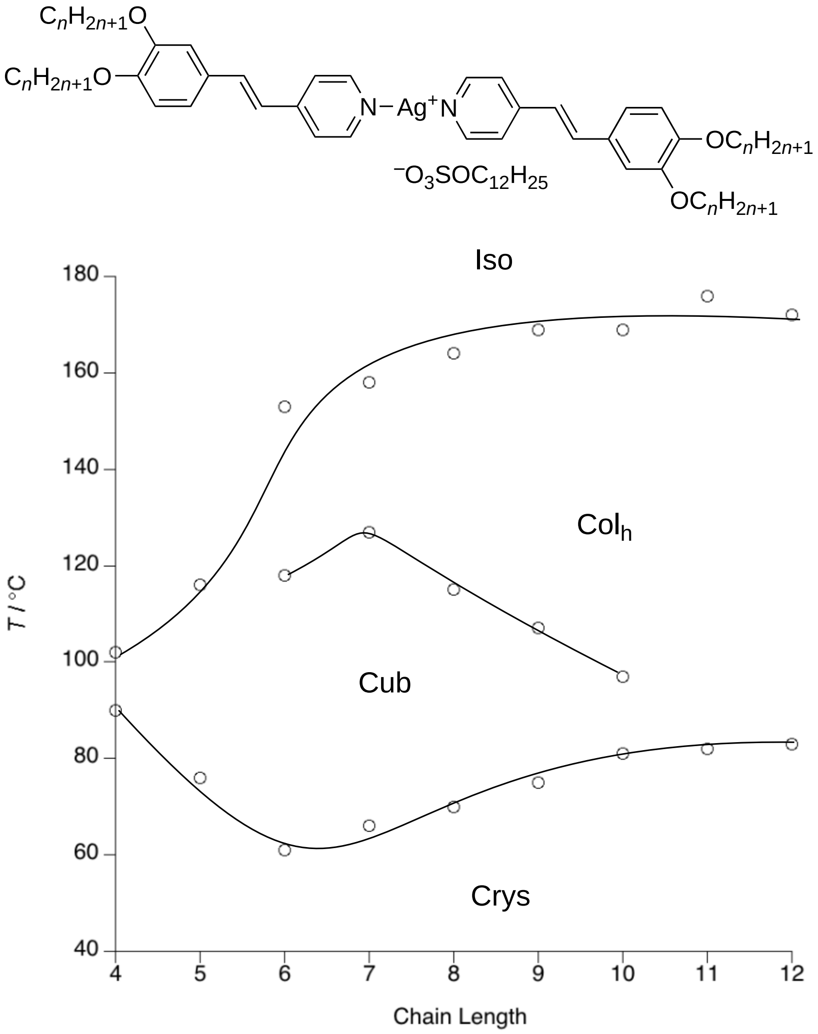

Figure S12. Phase diagram for tetracatenar silver(I) stilbazole dodecylsulfate complexes – re-drawn from data in B. Donnio, D. W. Bruce, B. Heinrich, D. Guillon, H. Delacroix and T. Gulik-Krzywicki, *Chem. Mater.,* **1997**, *9*, 2951-2961.